

One-loop proton decay from Peccei-Quinn symmetry

H. B. Câmara^{1,*}

¹*Institute of Experimental and Applied Physics,
Czech Technical University in Prague,
Prague 160 00, Czech Republic*

ABSTRACT

We promote the accidental $B+L$ symmetry of the Standard Model to a Peccei-Quinn (PQ) symmetry while realizing spontaneous proton decay radiatively. The PQ anomaly sector consists of vector-like quarks (VLQs), providing a Kim-Shifman-Vainshtein-Zakharov-type axion solution to the strong CP problem. After spontaneous PQ breaking, a residual \mathcal{Z}_2 symmetry remains, which forbids tree-level proton decay. The VLQs required to generate the QCD anomaly, together with scalar mediators, odd under the residual \mathcal{Z}_2 , induce one-loop proton decay through the effective operator $u_R u_R d_R e_R$. We study its ultraviolet completions, featuring distinct vector-like fermion and scalar representations, and show that the resulting models lead to distinct predictions for the axion-to-photon coupling, testable in helioscope and haloscope experiments. In addition to the proton decay channel $p \rightarrow e^+ \pi^0$, this framework predicts proton decay with an axion in the final state, $p \rightarrow e^+ \pi^0 a$, suppressed by the PQ-breaking scale. We also discuss axion dark matter in pre- and post-inflationary cosmology.

I. INTRODUCTION

Proton stability is ensured in the Standard Model (SM) by the accidental baryon number B and lepton number L symmetries. However, in the SM effective field theory, higher-dimensional operators consistent with the SM gauge symmetry generically violate B and L . Already at dimension five, the unique Weinberg operator $(\ell_L \Phi)(\ell_L \Phi)/\Lambda$, involving the lepton and Higgs doublet, where Λ is the typical new physics scale, violates lepton number by two units [1]. After electroweak (EW) symmetry breaking when Φ acquires a non-zero vacuum expectation value (VEV), this operator generates Majorana neutrino masses. At dimension six, the leading baryon-number-violating effects arise from four-fermion operators involving three quark fields and one lepton field $qqq\ell/\Lambda^2$ [1–5]. These operators mediate two-body nucleon decay processes that violate B and L each by one unit, implying $B+L$ violation by two units, while conserving $B-L$.

From an ultraviolet (UV) perspective, such operators arise naturally in Grand Unified Theories (GUTs) [6–8]. A prime example is the minimal $SU(5)$ GUT, where the exchange of heavy gauge bosons generates $qqq\ell/\Lambda^2$ at tree level [7]. These operators induce baryon-number-violating nucleon decay modes, most notably the golden channel $p \rightarrow e^+ \pi^0$ (for a recent review on B and L violation see Ref. [9]). Experimentally, Super-Kamiokande (Super-K), reports the most stringent bound on the partial proton mean lifetime: $\tau(p \rightarrow e^+ \pi^0) > 2.4 \times 10^{34}$ years at 90% CL [10]. This constraint pushes the GUT proton decay mediator mass scale to $\Lambda \sim \mathcal{O}(10^{16})$ GeV. Future large-volume detectors, including Hyper-Kamiokande (Hyper-K) [11], DUNE [12], and JUNO [13], are expected to substantially extend the sensitivity to nucleon decay and provide significantly improved probes of the $B+L$ -violating processes predicted in GUT scenarios.

* henrique.camara@cvut.cz

Proton decay may itself be predominantly a radiative phenomenon. Namely, Ref. [14] systematically classifies one-loop decomposition and UV completions of the dimension-six $B + L$ -violating operators $qqql/\Lambda^2$. In these scenarios, the mediators responsible for proton decay, such as scalar leptoquarks and/or vector-like quarks (VLQs), can lie at the TeV scale, opening the possibility of direct collider tests. Additionally, radiative proton-decay frameworks have been studied in connection to neutrino masses and dark matter (DM). In constructions based on the scotogenic idea [15, 16], the same dark-sector states responsible for generating neutrino masses radiatively can also mediate proton decay, linking the smallness of neutrino masses and the longevity of the proton [17, 18]. Furthermore, in Ref. [19], the accidental $B + L$ symmetry of the SM is promoted to a global $U(1)_{B+L}$ symmetry, which is subsequently spontaneously broken to a residual \mathcal{Z}_4 symmetry, stabilizing a viable weakly interacting massive particle (WIMP) DM candidate. Although proton decay is forbidden at tree level, it is generated via \mathcal{Z}_4 -odd mediators at one-loop.

Another longstanding issue of the SM concerns the strong CP phase $\bar{\theta}$, which encodes CP violation in Quantum Chromodynamics (QCD). Experimental searches for the neutron electric dipole moment impose the stringent bound $|\bar{\theta}| \lesssim 10^{-10}$ [20, 21], yet the SM offers no theoretical explanation for its smallness, giving rise to the strong CP problem. A particularly elegant solution relies on the Peccei-Quinn (PQ) mechanism [22, 23], which introduces a global QCD-anomalous $U(1)_{\text{PQ}}$ symmetry whose spontaneous breaking yields a pseudo-Goldstone boson, the axion [24, 25]. Non-perturbative QCD effects generate an axion potential whose minimum dynamically relaxes $\bar{\theta} \rightarrow 0$. The two paradigmatic invisible-axion frameworks are the Dine-Fischler-Srednicki-Zhitnitsky (DFSZ) [26, 27] and Kim-Shifman-Vainshtein-Zakharov (KSVZ) [28, 29] scenarios. In DFSZ models, SM quarks are chirally charged under PQ requiring an extra Higgs doublet in its minimal realization, whereas in KSVZ models the anomaly is generated by additional heavy VLQs. In both scenarios PQ-symmetry breaking is done via a scalar singlet σ allowing to decouple the PQ-breaking scale from the EW scale (for a review on axions see Ref. [30]).

Axion frameworks also offer a gateway to address multiple beyond the SM phenomena simultaneously. In particular, axion relics can be generated non-thermally in the early Universe such that axions account for the observed DM abundance [31–33]. Moreover, the axion-neutrino connection has been extensively explored. Namely, in type-I seesaw [34–39], where the VEV of a PQ-scalar σ , which sets the axion decay constant, also dynamically generates right-handed neutrino masses [40–48]. More recently, within the KSVZ framework, exotic colored vector-like fermions and scalar mediators have been employed to radiatively generate Majorana [49] and Dirac [50] neutrino masses. Furthermore, an axial version of $B + L$ global symmetry as a PQ symmetry has been studied within a DFSZ axion scenario where proton decay arises at tree-level [51].

Inspired by these ideas, in this work we promote the accidental global $B + L$ symmetry of the SM to a PQ symmetry, connecting proton stability to the axion solution of the strong CP problem, while realizing spontaneous proton decay radiatively. The PQ anomaly sector, composed of VLQs, solves the strong CP problem within the KSVZ axion scenario. After spontaneous PQ breaking, a residual \mathcal{Z}_2 symmetry remains, forbidding proton decay at tree level. The VLQs responsible for the QCD anomaly, together with scalar mediators, odd under a residual \mathcal{Z}_2 , induce proton decay at one-loop level. This paper is organized as follows. In Sec. II, we present the framework based on the symmetry-breaking pattern $U(1)_{\text{PQ}} \equiv U(1)_{B+L} \rightarrow \mathcal{Z}_2$, along with the particle content and their transformation properties under the SM gauge and PQ symmetries. We show how the proton decay operator $u_R u_R d_R e_R$ is generated spontaneously after PQ-breaking at one-loop and how the strong CP problem is addressed. In Sec. III, we study proton decay phenomenology, focusing on two-body channels such as $p \rightarrow e^+ \pi^0$ and their correlation with the PQ-breaking scale. We also comment on suppressed processes involving an axion in the final state, such as $p \rightarrow e^+ \pi^0 a$. The different models can be experimentally distinguished through their predictions for the axion-to-photon coupling, analyzed in Sec. IV, where we also discuss axion DM production in the early Universe. Finally, our concluding remarks are presented in Sec. V.

	Fields	$SU(3)_c \otimes SU(2)_L \otimes U(1)_Y$	$U(1)_{PQ} \equiv U(1)_{B+L} \rightarrow \mathcal{Z}_2$
Leptons	ℓ_L	$(\mathbf{1}, \mathbf{2}, -1/2)$	$1 \rightarrow +$
	e_R	$(\mathbf{1}, \mathbf{1}, -1)$	$1 \rightarrow +$
Quarks	q_L	$(\mathbf{3}, \mathbf{2}, 1/6)$	$1/3 \rightarrow +$
	d_R	$(\mathbf{3}, \mathbf{1}, -1/3)$	$1/3 \rightarrow +$
	u_R	$(\mathbf{3}, \mathbf{1}, 2/3)$	$1/3 \rightarrow +$
Scalars	Φ	$(\mathbf{1}, \mathbf{2}, 1/2)$	$0 \rightarrow +$
	σ	$(\mathbf{1}, \mathbf{1}, 0)$	$1 \rightarrow +$

TABLE I: Transformation properties under $SU(3)_c \otimes SU(2)_L \otimes U(1)_Y$ and $U(1)_{PQ}$, of the SM field content and σ which breaks the PQ symmetry into a residual \mathcal{Z}_2 (see text for details).

	Fields	$SU(3)_c$	$SU(2)_L$	$U(1)_Y$			$U(1)_{PQ} \equiv U(1)_{B+L} \rightarrow \mathcal{Z}_2$
				Case A	Case B	Case C	
Fermion	$\Psi_L; \Psi_R$	\mathbf{R}_Ψ	\mathbf{n}	Y_Ψ	Y_Ψ	Y_Ψ	$5/6; -1/6 \rightarrow -$
	$F_L; F_R$	\mathbf{R}_F	\mathbf{n}	$-Y_\Psi - 1/3$	$-Y_\Psi - 1/3$	$-Y_\Psi - 4/3$	$1/2; -1/2 \rightarrow -$
Scalar	S	\mathbf{R}_S	\mathbf{n}	$-Y_\Psi + 1/3$	$-Y_\Psi - 2/3$	$-Y_\Psi - 2/3$	$-1/6 \rightarrow -$
	χ	\mathbf{R}_χ	\mathbf{n}	$Y_\Psi - 2/3$	$Y_\Psi - 2/3$	$Y_\Psi + 1/3$	$1/2 \rightarrow -$

TABLE II: One-loop proton decay mediator fields Ψ, F, S, χ , and their transformation properties under $SU(3)_c \otimes SU(2)_L \otimes U(1)_Y$ and $U(1)_{PQ}$. The field σ presented in Table I, breaks $U(1)_{PQ}$ into \mathcal{Z}_2 . $\mathbf{R}_{\Psi, F, S, \chi}$ denote the $SU(3)_c$ representations of Table III. $SU(2)_L$ representation \mathbf{n} is common to all fields. Y_Ψ is the hypercharge of Ψ with three possible cases A, B and C for hypercharge assignments (see text for details).

II. FRAMEWORK

We identify the accidental global $B + L$ symmetry already present in the SM, where quark and lepton fields have charge $1/3$ and 1 , respectively, with the PQ symmetry responsible for solving the strong CP problem, i.e. $U(1)_{PQ} \equiv U(1)_{B+L}$. Besides the SM Higgs doublet $\Phi = (\phi^+, \phi^0)^T$, whose VEV $\langle \phi^0 \rangle = v$, breaks the EW symmetry and has no charge under PQ, we introduce a complex scalar singlet σ with charge 1 under $U(1)_{PQ}$. Once σ develops a non-zero VEV, the PQ symmetry is spontaneously broken at a scale $f_{PQ} = \langle \sigma \rangle$, into a residual discrete \mathcal{Z}_2 symmetry. As shown in Table I, the SM fields and σ are even under \mathcal{Z}_2 .

Furthermore, we introduce four fields consisting of two vector-like fermions, Ψ and F , and two scalars, S and χ , with transformation properties under the SM gauge and PQ symmetries shown in Table II. The fermions are chirally charged under $U(1)_{PQ}$, so that

$$\mathcal{L}_{PQ} = y_\Psi \overline{\Psi}_L \sigma \Psi_R + y_F \overline{F}_L \sigma F_R + \text{H.c.}, \quad (1)$$

and after PQ-symmetry breaking their masses are given by

$$M_\Psi = y_\Psi f_{PQ}, \quad M_F = y_F f_{PQ}. \quad (2)$$

Note that the $SU(2)_L$ representation $\mathbf{n} \equiv \mathbf{1}, \mathbf{2}, \mathbf{3}, \dots$, is common to all fields. Y_Ψ denotes the hypercharge of Ψ , and we consider three possible cases, A, B, and C, for the hypercharge assignments of the remaining fields. For the $SU(3)_c$ representations $\mathbf{R}_{\Psi, F, S, \chi}$, Table III lists all possible color contractions up to $\mathbf{R} \equiv \mathbf{8}$. As shown in the last column of Table II, the $U(1)_{PQ}$ charge assignments of Ψ, F, S , and χ are such that these fields are odd under the residual \mathcal{Z}_2 .

\mathbf{R}_Ψ	\mathbf{R}_F	\mathbf{R}_S	\mathbf{R}_χ	N/n
$\mathbf{1}$	$\mathbf{3}$	$\bar{\mathbf{3}}$	$\bar{\mathbf{3}}$	1
$\mathbf{3}$	$\mathbf{1}$	$\mathbf{3}$	$\mathbf{1}$	1
$\bar{\mathbf{3}}$	$\bar{\mathbf{3}}$	$\mathbf{1}$	$\mathbf{3}$	2
$\bar{\mathbf{3}}$	$\bar{\mathbf{3}}$	$\mathbf{8}$	$\mathbf{3}$	2
$\bar{\mathbf{3}}$	$\mathbf{6}$	$\mathbf{8}$	$\bar{\mathbf{6}}$	6
$\mathbf{6}$	$\bar{\mathbf{3}}$	$\mathbf{8}$	$\mathbf{3}$	6
$\mathbf{3}$	$\mathbf{8}$	$\mathbf{3}$	$\mathbf{8}$	7
$\mathbf{3}$	$\mathbf{8}$	$\bar{\mathbf{6}}$	$\mathbf{8}$	7
$\mathbf{8}$	$\mathbf{3}$	$\bar{\mathbf{3}}$	$\bar{\mathbf{3}}$	7
$\mathbf{8}$	$\mathbf{3}$	$\mathbf{3}$	$\bar{\mathbf{3}}$	7
$\bar{\mathbf{6}}$	$\mathbf{8}$	$\mathbf{3}$	$\mathbf{8}$	11
$\mathbf{8}$	$\bar{\mathbf{6}}$	$\bar{\mathbf{3}}$	$\mathbf{6}$	11

TABLE III: $SU(3)_c$ representations of the one-loop proton decay mediator fields Ψ, F, S, χ of Table II. Last column: color anomaly factor N/n values, where n is the dimension of the $SU(2)_L$ representation [see Eq. (10)].

For each case A, B, and C, the Yukawa Lagrangian contains the interactions

$$\mathcal{L}_A \supset \mathbf{Y}_1 \bar{d}_R^c S \Psi_R + \mathbf{Y}_2 \bar{u}_R \chi^\dagger \Psi_L + \mathbf{Y}_3 \bar{u}_R^c S^\dagger F_R + \mathbf{Y}_4 \bar{e}_R \chi F_L + \text{H.c.}, \quad (3)$$

$$\mathcal{L}_B \supset \mathbf{Y}_1 \bar{u}_R^c S \Psi_R + \mathbf{Y}_2 \bar{u}_R \chi^\dagger \Psi_L + \mathbf{Y}_3 \bar{d}_R^c S^\dagger F_R + \mathbf{Y}_4 \bar{e}_R \chi F_L + \text{H.c.}, \quad (4)$$

$$\mathcal{L}_C \supset \mathbf{Y}_1 \bar{u}_R^c S \Psi_R + \mathbf{Y}_2 \bar{d}_R \chi^\dagger \Psi_L + \mathbf{Y}_3 \bar{u}_R^c S^\dagger F_R + \mathbf{Y}_4 \bar{e}_R \chi F_L + \text{H.c.}, \quad (5)$$

where $\mathbf{Y}_{1,2,3,4}$ are 3×1 Yukawa vectors and for simplicity we omit the $SU(2)_L$ and $SU(3)_c$ indices. The most general scalar potential allowed by the symmetries of our framework can be written as

$$V = \sum_{\zeta} \left[\mu_{\zeta}^2 \zeta^\dagger \zeta + \lambda_{\zeta} (\zeta^\dagger \zeta)^2 \right] + \sum_{\zeta \neq \zeta'} \lambda_{\zeta \zeta'} (\zeta^\dagger \zeta) (\zeta'^\dagger \zeta'), \quad (6)$$

where $\zeta, \zeta' = \Phi, \sigma, S, \chi$.

As shown in Ref. [14], the fields Ψ, F, S , and χ , mediate at one-loop level the dimension-six operator $u_R u_R d_R e_R$. However, since $U(1)_{PQ}$ realizes $U(1)_{B+L}$, the operator $u_R u_R d_R e_R$ is forbidden because it violates PQ or equivalently $B + L$, by two units. Instead, the operator $u_R u_R d_R e_R \sigma^{*2}$ is generated at one-loop via the box diagram shown in Fig. 1, with $u_R u_R d_R e_R$ being spontaneously generated after PQ-symmetry breaking. Additionally, once the breaking pattern $U(1)_{PQ} \equiv U(1)_{B+L} \rightarrow \mathcal{Z}_2$ occurs, all SM fields, including u_R, d_R , and e_R , as well as σ , are even under the residual \mathcal{Z}_2 , whereas the mediator fields Ψ, F, S , and χ are odd (see last column of Table II). Although the proton decay operator $u_R u_R d_R e_R$ is not forbidden by the residual \mathcal{Z}_2 , as shown in Ref. [19] the even/odd character of the fields guarantees that proton decay cannot be generated at tree level¹. In Sec. III we will study the phenomenology of spontaneous one-loop proton decay, which is connected to the PQ-symmetry breaking.

The strong CP problem is solved within a KSVZ-type axion scenario since the vector-like fermions Ψ and F are chirally charged under the PQ symmetry as shown in Eq. (1). The PQ scalar field can be parametrized as,

$$\sigma = (f_{PQ} + \rho) \exp\left(\frac{ia}{f_{PQ}}\right), \quad (7)$$

where a is the axion and ρ is the radial mode. After spontaneous PQ breaking, the axion decay constant is

$$f_a = \frac{f_{PQ}}{N}, \quad (8)$$

¹ See Ref. [52] for an example in which discrete \mathcal{Z}_n symmetries are employed to forbid lower-dimensional proton decay operators.

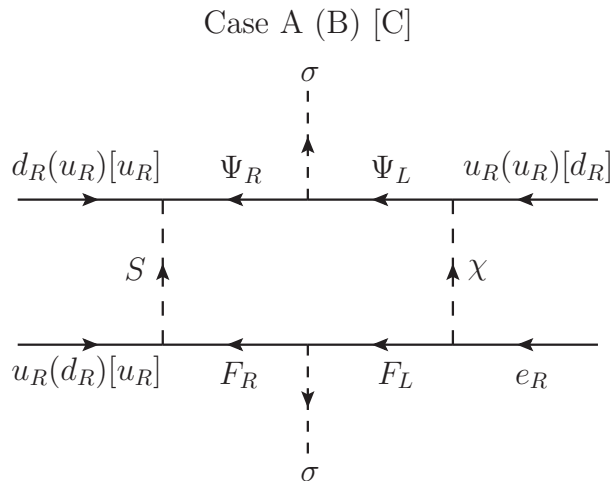


FIG. 1: One-loop box diagram generating the proton decay operator $u_R u_R d_R e_R \sigma^{*2}$ via the mediator fields Ψ, F, S, χ presented in Tables II and III (see text for details).

where N denotes the color anomaly factor. The up-to-date next-to-leading order (NLO) calculation of the axion mass yields [53]

$$m_a = 5.70(7) \left(\frac{10^{12} \text{GeV}}{f_a} \right) \mu\text{eV}. \quad (9)$$

This relation between m_a and f_a is a model-independent prediction of the QCD axion. Viability of the axion solution to the strong CP problem requires $N \neq 0$, ensuring an axion-gluon coupling. For the models in Tables II and III, we obtain

$$N = 2n [T(\mathbf{R}_\Psi) + T(\mathbf{R}_F)], \quad (10)$$

where n is the dimension of the $SU(2)_L$ representation \mathbf{n} and $T(\mathbf{R}_{\Psi,F})$ is the Dynkin index of the $SU(3)_c$ representation of Ψ, F . Hence, at least one of the vector-like fermions Ψ or F must transform nontrivially under $SU(3)_c$ in order to solve the strong CP problem. In Table III, for the possible $SU(3)_c$ representations $\mathbf{R}_{\Psi,F,S,\chi}$ up to $\mathbf{R} \equiv \mathbf{8}$, we report the corresponding values of N/n . Notice that in the cases $\mathbf{R}_\Psi \equiv \mathbf{1}$, $\mathbf{R}_F \equiv \mathbf{3}$ and $\mathbf{R}_\Psi \equiv \mathbf{3}$, $\mathbf{R}_F \equiv \mathbf{1}$, one of the vector-like fermions is a color singlet. In these situations, the color anomaly factor N is entirely determined by the other fermion. These cases also yield $N = 1$ if Ψ and F are $SU(2)_L$ singlets, with implications for axion DM that we briefly discuss in Sec. IV A. All remaining cases feature a PQ anomaly sector with two VLQs, Ψ and F , which also mediate proton decay at one loop, with the corresponding phenomenology discussed in the next section.

III. PROTON DECAY PHENOMENOLOGY

There are three possible hypercharge assignments for the fields Ψ, F, S , and χ , denoted in Table II as cases A, B, and C, which lead to distinct one-loop realizations of the operator $u_R u_R d_R e_R \sigma^{*2}$, as illustrated in Fig. 1. Once spontaneous breaking of the PQ symmetry is triggered by the VEV $\langle \sigma \rangle$, one-loop two-body proton and neutron decay processes are generated, as shown respectively in the top and bottom diagrams of Fig. 2. As shown in the top-left diagram, all cases A, B, and C give rise to the proton decay channels $p \rightarrow \ell^+ M^0$, where $\ell^+ = e^+, \mu^+$ and $M^0 = \pi^0, \eta, \rho^0, \omega$. In addition, case C also allows for the decay channel $p \rightarrow \ell^+ K^0$, as illustrated in the top-right diagram. Furthermore, the neutron decay channels $n \rightarrow \ell^+ \pi^-$ and $n \rightarrow \ell^+ \rho^-$ are also induced by cases A and B, as shown in the bottom diagram.

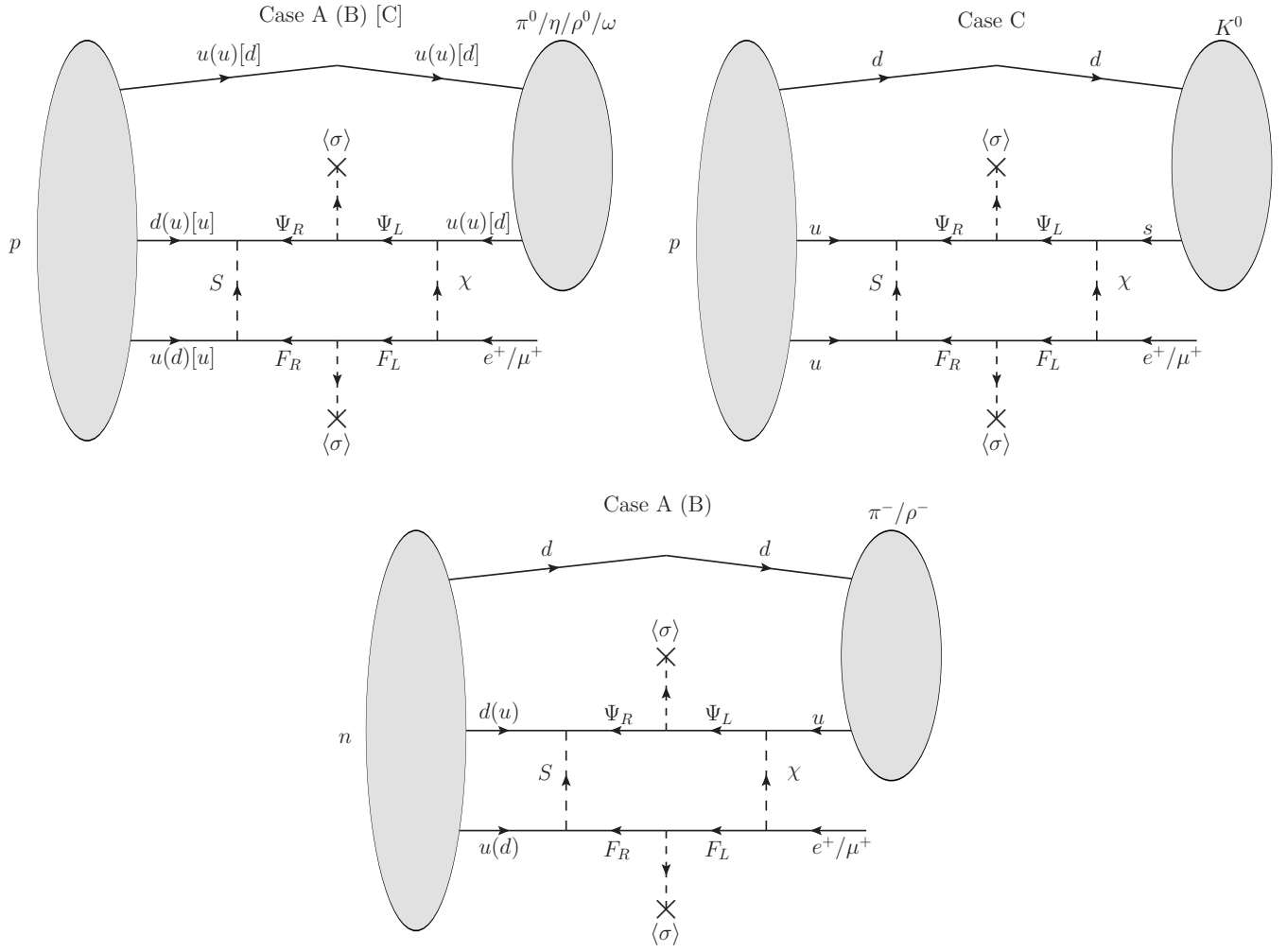


FIG. 2: One-loop proton (top) and neutron (bottom) two-body decays mediated by Ψ , F , S and χ (see Fig. 1 and text for details).

Decay mode	Partial mean lifetime ($\times 10^{33}$ years)	Allowed in Case
$p \rightarrow e^+\pi^0 / \mu^+\pi^0$	$> 24 / 14$ [10]	A, B, C
$p \rightarrow e^+\eta / \mu^+\eta$	$> 14 / 7.3$ [54]	
$p \rightarrow e^+\rho^0 / \mu^+\rho^0$	$> 0.72 / 0.57$ [55]	
$p \rightarrow e^+\omega / \mu^+\omega$	$> 1.6 / 2.8$ [55]	
$p \rightarrow e^+K^0 / \mu^+K^0$	> 1 [55] / 3.6 [56]	C
$n \rightarrow e^+\pi^- / \mu^+\pi^-$	$> 5.3 / 3.5$ [10]	A, B
$n \rightarrow e^+\rho^- / \mu^+\rho^-$	$> 0.217 / 0.228$ [55]	

TABLE IV: Partial mean lifetime limit for proton and neutron two-body decay modes allowed in our framework (see Fig. 2). All limits were obtained by the Super-K experiment at 90% CL.

In Table IV, we present the partial mean lifetime lower limits obtained by Super-K for the proton and neutron two-body decay modes allowed in our framework. Among them, the golden channel $p \rightarrow e^+\pi^0$ provides the most stringent constraint, with the current lower bound on the partial lifetime given by $\tau(p \rightarrow e^+\pi^0) > 2.4 \times 10^{34}$ years [10]. Future searches at Hyper-K are expected to significantly improve the sensitivity to proton decay, potentially extending the reach for the $p \rightarrow e^+\pi^0$ channel by about one order of magnitude in lifetime [11]. In what follows we focus on this paradigmatic proton decay channel and then comment on the other processes.

As a benchmark scenario to study $p \rightarrow e^+\pi^0$, and without loss of generality, we consider a concrete realization of our framework. In particular, we focus on case A with $Y_\Psi = 0$ and, for simplicity, take the $SU(2)_L$ representation to be $\mathbf{n} \equiv \mathbf{1}$ (see Table II). For the $SU(3)_c$ representations, we likewise consider the simplest scenario involving only two colored mediators, namely $\mathbf{R}_\Psi \equiv \mathbf{3}$ and $\mathbf{R}_F \equiv \mathbf{1}$ for the fermionic sector, together with $\mathbf{R}_S \equiv \mathbf{3}$ and $\mathbf{R}_\chi \equiv \mathbf{1}$ for the scalar sector (see Table III). The vector-like fermion masses are dynamically generated through PQ-symmetry breaking, as given in Eq. (2). Furthermore, from the scalar potential in Eq. (6), the scalar masses of S and χ are obtained as

$$M_S^2 = \mu_S^2 + \lambda_{\Phi S} v^2 + \lambda_{\sigma S} f_{\text{PQ}}^2, \quad M_\chi^2 = \mu_\chi^2 + \lambda_{\Phi \chi} v^2 + \lambda_{\sigma \chi} f_{\text{PQ}}^2. \quad (11)$$

Since both S and χ are electrically charged, and S is additionally colored, neither field can acquire a VEV in order to preserve electromagnetism and color. This requirement implies that the quadratic parameters must satisfy $\mu_{S,\chi}^2 > 0$.

The proton decay width induced at one-loop level for the two-body mode $p \rightarrow e^+\pi^0$ can be written as

$$\Gamma(p \rightarrow e^+\pi^0) = \frac{m_p}{32\pi} \left(1 - \frac{m_{\pi^0}^2}{m_p^2}\right)^2 |W_0 \mathcal{C}|^2, \quad (12)$$

with the proton and neutral pion masses being $m_p = 0.938$ GeV and $m_{\pi^0} = 0.135$ GeV, respectively [57]. Since we radiatively generate the operator $u_R u_R d_R e_R \sigma^{*2}$, the value of the hadronic matrix element above is $W_0 = -0.131$ GeV² [58]. The loop factor \mathcal{C} is [14],

$$\mathcal{C} = -|Y_1 Y_2 Y_3 Y_4| M_\Psi M_F \mathcal{I}(M_\Psi, M_F, M_S, M_\chi), \quad (13)$$

where the Yukawa couplings $Y_{1,2,3,4}$ correspond to the first-generation fermion entries of the Yukawa vectors $\mathbf{Y}_{1,2,3,4}$ of Eq. (3). The box-diagram loop integral \mathcal{I} (see Figs. 1 and 2), is a function of the mediator masses M_Ψ, M_F and M_S, M_χ , given by Eqs. (2) and (11), respectively. The proton decay partial mean lifetime is obtained through,

$$\tau(p \rightarrow e^+\pi^0) = \frac{1}{\Gamma(p \rightarrow e^+\pi^0)}. \quad (14)$$

The framework considered here is an invisible KSVZ-axion scenario, where the PQ symmetry is identified as $B+L$. Once the PQ-symmetry, and therefore $B+L$, is spontaneously broken one-loop proton decay is generated. The PQ-breaking scale $f_{\text{PQ}} = \langle \sigma \rangle$ is typically of order 10^{12} GeV [see Eq. (9)], and thus lies many orders of magnitude above the EW scale, $f_{\text{PQ}} \gg v \simeq 246$ GeV. As will be discussed in Sec. IV A and shown in Fig. 3, such a PQ scale naturally allows axions to account for the observed DM relic abundance. Consequently, due to the connection between PQ-symmetry breaking and $B+L$ violation, the proton decay mediator fields Ψ, F, S , and χ are expected to acquire masses of order f_{PQ} [see Eqs. (2) and (11)]. In the limit where all masses in the loop are heavy compared to external momenta and identical $M_\Psi = M_F = M_S = M_\chi \equiv M$, the loop integral is given by,

$$\mathcal{I}(M) \simeq \frac{1}{16\pi^2} \frac{1}{6M^4}. \quad (15)$$

In this limit we obtain the parametric expression for the proton decay lifetime

$$\tau(p \rightarrow e^+\pi^0) \simeq 10^{34} \text{ years} \left(\frac{10^{-4}}{Y_1 Y_2 Y_3 Y_4} \right)^2 \left(\frac{M}{10^{12} \text{ GeV}} \right)^4. \quad (16)$$

The above expression is a reasonable approximation since $M_\Psi \sim M_F \sim M_S \sim M_\chi \sim \mathcal{O}(f_{\text{PQ}}) \gg v$, for $y_{\Psi,F} \sim \mathcal{O}(1)$ and $\lambda_{\sigma S,\chi} \sim \mathcal{O}(1)$. We note that, in order to satisfy the Super-K constraint shown in Table IV, for $M \simeq f_{\text{PQ}} \simeq 10^{12}$ GeV, the Yukawa combination must satisfy $Y_1 Y_2 Y_3 Y_4 \lesssim 10^{-4}$. Therefore, taking all aforementioned Yukawa and scalar quartic couplings to lie in the range $\mathcal{O}(0.1-1)$ easily satisfies the stringent proton decay bounds at the typical PQ scale of 10^{12} GeV. This follows from the intimate connection between PQ-symmetry breaking and $B+L$ violation, together with the fact that proton decay is generated at one loop, leading to an additional suppression of the decay rate and consequently an enhancement of the corresponding lifetime. Our situation contrasts with Refs. [14, 19], where by suppressing the Yukawa combination $Y_1 Y_2 Y_3 Y_4$ down to values below 10^{-20} , which corresponds to individual couplings smaller than 10^{-5} , allows for the mediator masses to lie at the TeV scale, leading to interesting phenomenological implications such as viable WIMP DM candidates and testable collider signatures. In our framework, however, DM is provided by the axion (see Sec. IV A) and the VLQs and scalar leptoquarks are expected to lie far beyond the direct reach of collider experiments. Lowering their masses to the TeV scale, so as to make them accessible at colliders, would require unnaturally small Yukawa couplings, $y_{\Psi,F} \sim \mathcal{O}(10^{-9})$, and/or scalar quartic couplings, $\lambda_{\sigma S,\chi} \sim \mathcal{O}(10^{-18})$. Nevertheless, as we will show in Sec. IV B, the different mediator field representations listed in Tables II and III can still be distinguished indirectly through their distinct predictions for the axion-to-photon coupling.

Regarding the other decay channels in Fig. 2, which are currently less constrained than $p \rightarrow e^+ \pi^0$ as indicated in Table IV, a detailed analysis would lead to conclusions qualitatively similar to those obtained for the $p \rightarrow e^+ \pi^0$ channel. Nevertheless, it is important to emphasize that some of these decay modes provide complementary probes of the same underlying interactions, while others are sensitive to additional Yukawa couplings. In particular, for cases A, B, and C, the decay channels $p \rightarrow e^+ \eta$, $p \rightarrow e^+ \rho^0$, and $p \rightarrow e^+ \omega$, shown in the top-left diagram, as well as, for cases A and B, the neutron decay modes $n \rightarrow e^+ \pi^-$ and $n \rightarrow e^+ \rho^-$ shown in the bottom diagram, probe the same combination of Yukawa couplings $Y_{1,2,3,4}$ as $p \rightarrow e^+ \pi^0$, corresponding to the first-generation fermion entries of the Yukawa vectors $\mathbf{Y}_{1,2,3,4}$ appearing in Eqs. (3), (4), and (5). On the other hand, channels involving μ^+ are sensitive to the second-generation entry of the Yukawa vector \mathbf{Y}_4 . Furthermore, in case C, the decay channels $p \rightarrow e^+ K^0$ and $p \rightarrow \mu^+ K^0$ are also allowed, probing the second-generation entry of the Yukawa vector \mathbf{Y}_2 in Eq. (5).

Lastly, since PQ-symmetry breaking lies at the origin of $B+L$ violation, triggering spontaneous one-loop proton decay, our framework naturally predicts exotic proton decay channels with an axion in final state, such as $p \rightarrow e^+ \pi^0 a$ and $p \rightarrow e^+ \pi^0 aa$. Namely, using Eq. (7) and expanding the σ field, we obtain

$$\frac{\mathcal{C}}{f_{\text{PQ}}^2} u_R u_R d_R e_R \sigma^{*2} \rightarrow \mathcal{C} u_R u_R d_R e_R \left(1 - \frac{2ia}{f_{\text{PQ}}} - \frac{2a^2}{f_{\text{PQ}}^2} + \dots \right), \quad (17)$$

where the same loop coefficient \mathcal{C} defined in Eq. (13), which controls the standard two-body decay $p \rightarrow e^+ \pi^0$, also determines the effective couplings associated with one and two axion emission. Although the axion appears here through non-derivative interactions, this description is equivalent, after a standard PQ rotation of the fermion fields, to the usual derivative coupling of the axion to fermions as a pseudo-Goldstone boson². Consequently, axion-emission amplitudes are effectively controlled by the characteristic momentum transfer of the process, namely $p \sim m_p$. For the typical invisible-axion scale $f_{\text{PQ}} \sim \mathcal{O}(10^{12})$ GeV, these exotic channels are therefore expected to be extremely suppressed. In particular, the decay widths satisfy the hierarchy

$$\frac{\Gamma(p \rightarrow e^+ \pi^0 a a)}{\Gamma(p \rightarrow e^+ \pi^0 a)} \sim \frac{\Gamma(p \rightarrow e^+ \pi^0 a)}{\Gamma(p \rightarrow e^+ \pi^0)} \sim \frac{1}{16\pi^2} \left(\frac{m_p}{f_{\text{PQ}}} \right)^2 \sim \mathcal{O}(10^{-27}) \ll 1, \quad (18)$$

where each emitted axion introduces an additional suppression factor $\sim m_p/f_{\text{PQ}}$ in the amplitude, while the multi-body final states are further suppressed by the usual phase-space factor $\sim 1/16\pi^2$. Consequently, from the above it is clear that the standard two-body proton decay modes dominate over the channels with axions in the final state.

² For comprehensive studies of baryon-number-violating decays involving axions and axion-like particles from an effective field theory perspective, see Refs. [59, 60].

IV. AXION PHENOMENOLOGY

A. Axion dark matter and cosmology

Axions are naturally light, weakly coupled to ordinary matter, nearly stable, and can be non-thermally produced in the early Universe, providing an excellent DM candidate. Axion DM production depends on whether the PQ symmetry breaks before or after inflation. We briefly discuss both possibilities below.

In the pre-inflationary scenario, the PQ symmetry is broken before inflation. In this case, axion DM is generated entirely through the misalignment mechanism [31–33]. The relic axion abundance can be approximately written as [30]

$$\Omega_a h^2 \simeq \Omega_{\text{DM}} h^2 \left(\frac{\theta_0}{2.15} \right)^2 \left(\frac{f_a}{2 \times 10^{11} \text{ GeV}} \right)^{\frac{7}{6}}, \quad (19)$$

where $|\theta_0| \in [0, \pi)$ denotes the initial misalignment angle and the observed cold DM relic abundance, obtained by Planck satellite data is $\Omega_{\text{DM}} h^2 = 0.1200 \pm 0.0012$ [61]. Hence, for $0.1 < \theta_0 < \pi$ the axion decay constant needs to be $10^{11} \text{ GeV} < f_a < 4 \times 10^{13} \text{ GeV}$, in order for axions to account for all the observed DM relic abundance. As discussed in Sec. IV B and shown in Fig. 3, this parameter space region is currently being probed by haloscope experiments. In this scenario, the axion leaves an imprint in primordial fluctuations, reflected in the cosmic microwave background (CMB) anisotropies and large-scale structure. The resulting isocurvature fluctuations are constrained by CMB data [62], leading to an upper bound on the inflationary scale H_I [63]:

$$H_I \lesssim \frac{0.9 \times 10^7}{\Omega_a h^2 / \Omega_{\text{DM}} h^2} \left(\frac{\theta_0}{\pi} \frac{f_a}{10^{11} \text{ GeV}} \right) \text{ GeV}. \quad (20)$$

Taking $\theta_0 \sim \mathcal{O}(1)$ and $\Omega_a h^2 = 0.12$, leads to a low scale for inflation $H_I \lesssim 10^7 \text{ GeV}$, with Planck currently probing $H_I \lesssim 10^{13} \text{ GeV}$ [61]. Nonetheless, the isocurvature bound depends on the UV completion and on the specific inflationary mechanism at play, and can therefore be relaxed in concrete scenarios [64]. In this work, however, we do not specify an explicit inflationary setup in which this CMB constraint can be consistently assessed. A dedicated study of inflation in such KFSZ models is left for future work, along the lines of Refs. [46, 47].

In the post-inflationary scenario, the PQ symmetry is broken after inflation, resulting in an observable Universe composed of patches with different initial values of the axion field. Consequently, the initial misalignment angle θ_0 is no longer a free parameter, but is instead statistically determined, with the current estimate $\langle \theta_0^2 \rangle \simeq 2.15^2$ [30]. This makes the scenario, in principle, more predictive than the pre-inflationary case. Requiring $\Omega_a h^2 = \Omega_{\text{DM}} h^2$ then fixes the axion scale f_a (or equivalently m_a) [see Eq. (19)]. If the axion abundance arises solely from the misalignment mechanism, avoiding DM overproduction implies $f_a \lesssim 2 \times 10^{11} \text{ GeV}$. However, the situation is more involved since topological defects, namely axion strings and domain walls (DWs), also contribute to the total relic abundance $\Omega_a h^2$ [65–68]. The non-linear evolution of the resulting DW-string network must be studied numerically, and its precise contribution remains an open question. A detailed analysis lies beyond the scope of this work. Nonetheless, the cosmological DW problem is absent for $N_{\text{DW}} = N = 1$. N_{DW} denotes the vacuum degeneracy of the axion potential associated with the residual \mathcal{Z}_N symmetry left unbroken by QCD instanton effects that anomalously break $U(1)_{\text{PQ}}$. This occurs for the models in Tables II and III, where Ψ and F are $SU(2)_L$ singlets, i.e. $\mathbf{n} = 1$, with their $SU(3)_c$ representations consisting of one being a color triplet $\mathbf{3}$ while the other is a color singlet $\mathbf{1}$. All other cases lead to DW formation in the early Universe [69]. Even for $N_{\text{DW}} = 1$, axionic string networks can still form. Numerical simulations indicate that reproducing the observed DM abundance, $\Omega_a h^2 = \Omega_{\text{DM}} h^2$, requires $f_a \in [5 \times 10^9, 3 \times 10^{11}] \text{ GeV}$ [70–74]. Even in scenarios with $N_{\text{DW}} > 1$, one may introduce small bias terms in the scalar potential that explicitly break the residual \mathcal{Z}_N symmetry of the axion potential. This lifts the vacuum degeneracy and renders the DW-string network unstable [75]. The subsequent decay of strings and DWs may then generate potentially observable stochastic gravitational wave signals [76–78].

Case A/B (Case C): E/N values for $Y_\Psi = 0$				
SU(3) _c		SU(2) _L		
\mathbf{R}_Ψ	\mathbf{R}_F	1	2	3
1	3	2/3 (32/3)	8/3 (38/3)	6 (16)
3	1	2/9 (32/9)	20/9 (50/9)	50/9 (80/9)
$\bar{\mathbf{3}}$	$\bar{\mathbf{3}}$	1/3 (16/3)	11/6 (41/6)	13/3 (28/3)
$\bar{\mathbf{3}}$	6	2/9 (32/9)	35/36 (155/36)	20/9 (50/9)
6	$\bar{\mathbf{3}}$	1/9 (16/9)	31/36 (91/36)	19/9 (34/9)
3	8	16/63 (256/63)	131/126 (611/126)	148/63 (388/63)
8	3	2/21 (32/21)	37/42 (97/42)	46/21 (76/21)
$\bar{\mathbf{6}}$	8	16/99 (256/99)	79/99 (29/9)	184/99 (424/99)
8	$\bar{\mathbf{6}}$	4/33 (64/33)	25/33 (85/33)	20/11 (40/11)

TABLE V: E/N values for $Y_\Psi = 0$, for Case A/B (Case C) – see Tables II and III and Eqs. (22) and (23).

The one-loop proton decay mediators Ψ , F , S , and χ are odd under \mathcal{Z}_2 . As a consequence, the lightest \mathcal{Z}_2 -odd state is stable and can be thermally produced after inflation. This may lead to cosmological problems, particularly if the lightest state among Ψ , F , S , and χ is colored and/or electrically charged [79–81]. Indeed, searches in terrestrial, lunar, and meteoritic materials place stringent bounds on such stable baryonic and/or charged relics [80–84], excluding them unless some mechanism suppresses their abundance or allows them to decay into ordinary matter [63, 79, 85]. Among the mediator representations listed in Tables II and III, the problematic stable relics can be avoided in scenarios where either Ψ or F is a fermionic SM singlet, or where S or χ is a scalar SM singlet. In fact, Ref. [19] exploits a global $B + L$ symmetry broken to a residual \mathcal{Z}_4 symmetry to stabilize a viable WIMP DM candidate corresponding to either a fermionic or scalar singlet mediator participating in one-loop proton decay. In our framework, taking Ψ , F , S , and χ to be SU(2)_L singlets allows for scenarios containing either one fermionic or scalar SM singlet. The fermionic singlet scenario, $\Psi \sim (\mathbf{1}, \mathbf{1}, 0)$ is obtained for $Y_\Psi = 0$ together with $\mathbf{R}_\Psi \equiv \mathbf{1}$. As shown in Table III, this implies $\mathbf{R}_F \equiv \mathbf{3}$ and $\mathbf{R}_S = \mathbf{R}_\chi \equiv \bar{\mathbf{3}}$, leading to $N_{\text{DW}} = 1$. Alternatively, $F \sim (\mathbf{1}, \mathbf{1}, 0)$ is realized by taking $Y_\Psi = -1/3$ for cases A and B, or $Y_\Psi = -4/3$ for case C, together with $\mathbf{R}_F \equiv \mathbf{1}$. This implies $\mathbf{R}_\Psi = \mathbf{R}_S \equiv \mathbf{3}$ and $\mathbf{R}_\chi \equiv \mathbf{1}$, again yielding $N_{\text{DW}} = 1$. The scalar singlet scenario, $\chi \sim (\mathbf{1}, \mathbf{1}, 0)$ is obtained by taking $Y_\Psi = 2/3$ for cases A and B, or $Y_\Psi = -1/3$ for case C, together with $\mathbf{R}_\chi \equiv \mathbf{1}$. In this case $\mathbf{R}_\Psi = \mathbf{R}_S \equiv \mathbf{3}$ and $\mathbf{R}_F \equiv \mathbf{1}$, also leading to $N_{\text{DW}} = 1$. Consequently, the more predictive post-inflationary axion scenario becomes viable for these cases. By contrast, the $S \sim (\mathbf{1}, \mathbf{1}, 0)$ scenario leads to $N_{\text{DW}} = 2$ (see Table III), and therefore inevitably suffers from the cosmological DW problem. For the majority of models within our framework, it is therefore judicious to assume a pre-inflationary axion DM scenario. In fact, since the breaking of U(1)_{PQ} occurs before inflation, axionic strings, DWs, and any primordial abundance of stable baryonic and/or charged relics will be washed out during inflation.

B. Axion-to-photon coupling

The various models presented in Tables II and III can be probed experimentally via their predictions for the axion-to-photon coupling $g_{a\gamma\gamma}$. NLO chiral Lagrangian techniques provide the following result [53]

$$g_{a\gamma\gamma} = \frac{\alpha_e}{2\pi f_a} \left[\frac{E}{N} - 1.92(4) \right], \quad (21)$$

where $\alpha_e = e^2/(4\pi)$, and the ratio E/N is the model-dependent contribution, with E being the electromagnetic anomaly factor.

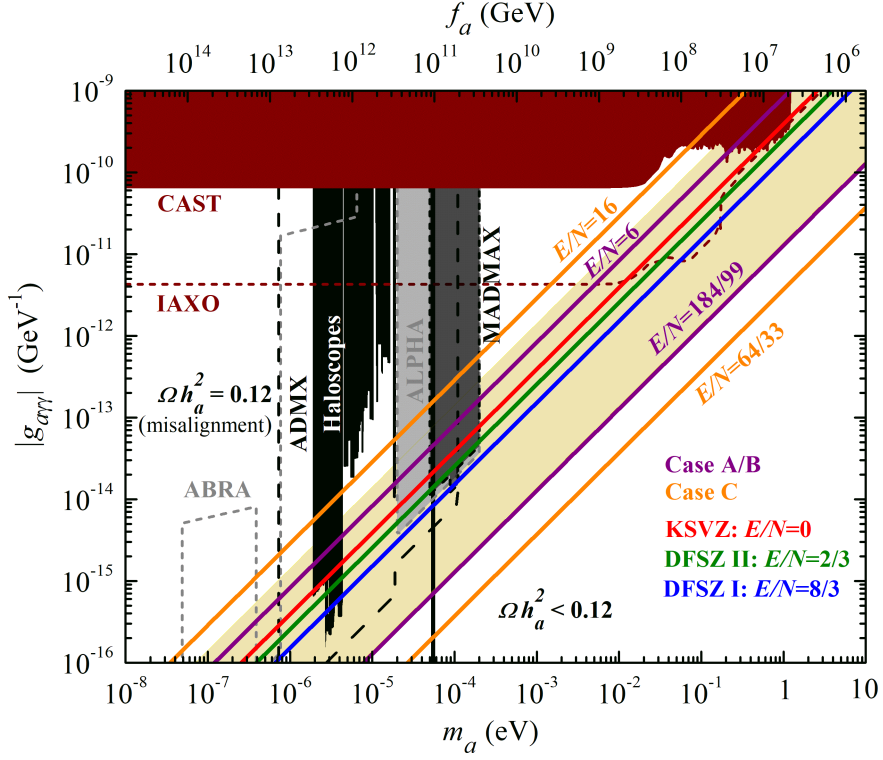


FIG. 3: Axion-to-photon coupling $|g_{a\gamma\gamma}|$ versus axion mass m_a (bottom axis) and decay constant f_a (top axis). The purple (orange) lines correspond to E/N values leading to maximum and minimum $|g_{a\gamma\gamma}|$ for case A/B (C) given the representations shown in Table V. The KSVZ and DFSZ I and II predictions are indicated by the red, blue, and green lines, respectively. The yellow shaded region refers to the usual QCD axion window [63]. Current constraints from helioscopes like CAST [86] exclude the bordeaux shaded region, while haloscopes like ADMX [87–89], RBF [90], CAPP [91] and HAYSTAC [92], rule out the black region. Projected sensitivities of IAXO [93], ADMX [94], MADMAX [95], ALPHA [96] and ABRACADABRA [97] are indicated by the dashed bordeaux, dashed black, short-dash black (dark-gray shaded region), dotted (light-gray shaded region) and gray-dashed contours, respectively. To the right of the black vertical line, axion DM is underabundant $\Omega h_a^2 < 0.12$. In the left region $\Omega h_a^2 = 0.12$, for the pre-inflationary case with axion DM produced via the misalignment mechanism.

As shown in Table II, the allowed hypercharge assignments for the one-loop proton-decay mediators Ψ , F , S , and χ fall into three classes, labelled A, B, and C. Cases A and B yield identical hypercharges for the vector-like fermions Ψ and F , whereas case C leads to a distinct assignment. Moreover, since all mediators share the same $SU(2)_L$ representation, there are only two independent expressions for E , namely

$$E_{A/B} = 2 \sum_{j=0}^{n-1} \left[d(\mathbf{R}_\Psi) \left(j - \frac{n-1}{2} + Y_\Psi \right)^2 + d(\mathbf{R}_F) \left(j - \frac{n-1}{2} - Y_\Psi - \frac{1}{3} \right)^2 \right], \quad (22)$$

$$E_C = 2 \sum_{j=0}^{n-1} \left[d(\mathbf{R}_\Psi) \left(j - \frac{n-1}{2} + Y_\Psi \right)^2 + d(\mathbf{R}_F) \left(j - \frac{n-1}{2} - Y_\Psi - \frac{4}{3} \right)^2 \right], \quad (23)$$

where $d(\mathbf{R}_{\Psi,F})$ is the dimension of the $SU(3)_c$ representation of Ψ, F . The quantities in parentheses correspond to the electric charges of the individual components of the $SU(2)_L$ multiplets Ψ and F . Consequently, for fixed Y_Ψ and \mathbf{n} , cases A and B give identical model-dependent contributions to $g_{a\gamma\gamma}$. In Table V we list the resulting E/N values for $Y_\Psi = 0$, entries are given for case A/B, with the corresponding case C values shown in parentheses. We include all allowed $SU(3)_c$ representations of Ψ and F shown in Table III, and consider $SU(2)_L$ multiplets up to $\mathbf{n} \equiv 3$.

In Fig. 3 we show $|g_{a\gamma\gamma}|$ as a function of the axion mass m_a (bottom axis) and decay constant f_a (top axis) [see Eq. (9)]. The benchmark KSVZ (hadronic) [28, 29] and DFSZ-I/II [26, 27] predictions are indicated by the solid red, blue, and green curves, respectively. The yellow band denotes the standard QCD-axion range $|E/N - 1.92| \in [0.07, 7]$ [63]. The purple (orange) lines delimit the maximum and minimum $|g_{a\gamma\gamma}|$ obtained in case A/B (C), for the mediator representations listed in Table V. For case A/B [C], the largest coupling corresponds to $E/N = 6$ [$E/N = 16$], realized by $\Psi \sim (\mathbf{1}, \mathbf{3}, 0)$ and $F \sim (\mathbf{3}, \mathbf{3}, -1/3)$ [$F \sim (\mathbf{3}, \mathbf{3}, -4/3)$] (see Tables II and III). The smallest coupling occurs for $E/N = 184/99$ [$E/N = 64/33$], realized by $\Psi \sim (\bar{\mathbf{6}}, \mathbf{3}, 0)$ and $F \sim (\mathbf{8}, \mathbf{3}, -1/3)$ [$\Psi \sim (\mathbf{8}, \mathbf{1}, 0)$ and $F \sim (\bar{\mathbf{6}}, \mathbf{1}, -4/3)$].

In the figure we show the current bounds and projected sensitivities from helioscopes and haloscopes. The CAST [86] helioscope experiment excludes the bordeaux-shaded region, while IAXO is expected to reach $g_{a\gamma\gamma} \sim (10^{-12} - 10^{-11}) \text{ GeV}^{-1}$ and probe the benchmark QCD-axion models (red, green and blue lines) around $m_a \sim 0.1 \text{ eV}$ (bordeaux dashed contour). Haloscopes target non-relativistic axions, assuming they constitute DM. As discussed in Sec. IV A, the misalignment mechanism yields the observed DM relic abundance only to the left of the black vertical line [see Eq. (19)], while to the right, axions are underabundant. The haloscopes, ADMX [87–89], RBF [90], CAPP [91], and HAYSTAC [92] exclude the black-shaded region. Among these, ADMX has already reached the KSVZ (red line) and DFSZ (blue/green line) predictions near $m_a \sim 3 \mu\text{eV}$, and the forthcoming ADMX generations (black dashed contour) aim for sensitivities down to $g_{a\gamma\gamma} \sim 10^{-16} \text{ GeV}^{-1}$ over $1 \mu\text{eV} \lesssim m_a \lesssim 100 \mu\text{eV}$. In addition, ALPHA [96, 98, 99] (light-gray band) and MADMAX [95] (dark-gray band) are projected to cover $20 \mu\text{eV} \lesssim m_a \lesssim 120 \mu\text{eV}$ and $50 \mu\text{eV} \lesssim m_a \lesssim 120 \mu\text{eV}$, respectively. Finally, ABRACADABRA [97] (gray dashed contour) is expected to probe $m_a \lesssim 1 \mu\text{eV}$ and reach the yellow shaded QCD-axion band.

V. CONCLUDING REMARKS

In this work, we propose a framework in which the PQ symmetry is identified with $B + L$ symmetry, such that proton decay is generated at one-loop level through the exchange of vector-like fermions Ψ , F and scalar mediators S , χ , as shown in Figs. 1 and 2. The PQ anomaly sector, composed of the vector-like fermions Ψ and F , chirally charged under $U(1)_{\text{PQ}}$, solves the strong CP problem within a KSVZ-type axion framework. After spontaneous PQ-symmetry breaking, a residual \mathcal{Z}_2 symmetry remains unbroken, under which the mediator fields Ψ , F , S , and χ are odd, guaranteeing that proton decay is forbidden at tree level.

We study UV completions of the operator $u_R u_R d_R e_R \sigma^{*2}$, which, after PQ-symmetry breaking, when σ acquires a non-zero VEV, induces proton decay at one loop. Different realizations, characterized by distinct vector-like fermion and scalar representations under the SM gauge group, lead to different proton and neutron decay channels shown in Fig. 2 and summarized in Table IV. In addition to the standard channel $p \rightarrow e^+ \pi^0$, the framework predicts axion-emitting modes such as $p \rightarrow e^+ \pi^0 a$, though these are strongly suppressed by the PQ-breaking scale.

Different representation assignments of the mediator fields Ψ , F , S and χ under the SM gauge group lead to distinct predictions for the axion-to-photon coupling. This allows to experimentally distinguish the different realizations of our framework at haloscope and helioscope experiments such as IAXO, ADMX, and MADMAX, as shown in Fig. 3.

We also discuss axion DM in pre- and post-inflationary cosmological scenarios. Due to the residual \mathcal{Z}_2 symmetry, the lightest odd field among Ψ , F , S and χ can yield long-lived colored and/or electrically charged relics. Furthermore, most realizations have a DW number $N_{\text{DW}} > 1$, which would produce axion string and DW networks, motivating a pre-inflationary scenario where such defects are inflated away. In this case, axions can account for the observed cold DM abundance for $\theta_0 \sim \mathcal{O}(1)$ and $f_a \sim 5 \times 10^{11} \text{ GeV}$, via the misalignment mechanism.

In summary, our framework promotes the accidental global $B + L$ symmetry already present in the SM to a PQ symmetry, thereby connecting the stability of the proton with the axion solution to the strong CP problem.

ACKNOWLEDGMENTS

HBC would like to thank F.R. Joaquim and R. Srivastava for carefully reading the manuscript and for helpful suggestions, as well as J. R. Rocha for valuable discussions. HBC thanks CFTP (Lisbon) for hospitality and financial support during the final stage of this work.

-
- [1] S. Weinberg, “Baryon and Lepton Nonconserving Processes,” *Phys. Rev. Lett.* **43** (1979) 1566–1570.
- [2] F. Wilczek and A. Zee, “Operator Analysis of Nucleon Decay,” *Phys. Rev. Lett.* **43** (1979) 1571–1573.
- [3] L. F. Abbott and M. B. Wise, “The Effective Hamiltonian for Nucleon Decay,” *Phys. Rev. D* **22** (1980) 2208.
- [4] A. Kobach, “Baryon Number, Lepton Number, and Operator Dimension in the Standard Model,” *Phys. Lett. B* **758** (2016) 455–457, [arXiv:1604.05726 \[hep-ph\]](#).
- [5] B. Grzadkowski, M. Iskrzynski, M. Misiak, and J. Rosiek, “Dimension-Six Terms in the Standard Model Lagrangian,” *JHEP* **10** (2010) 085, [arXiv:1008.4884 \[hep-ph\]](#).
- [6] J. C. Pati and A. Salam, “Unified Lepton-Hadron Symmetry and a Gauge Theory of the Basic Interactions,” *Phys. Rev. D* **8** (1973) 1240–1251.
- [7] H. Georgi and S. L. Glashow, “Unity of All Elementary Particle Forces,” *Phys. Rev. Lett.* **32** (1974) 438–441.
- [8] H. Fritzsch and P. Minkowski, “Unified Interactions of Leptons and Hadrons,” *Annals Phys.* **93** (1975) 193–266.
- [9] V. Takhistov, “Experimental Tests of Baryon and Lepton Number Conservation,” [arXiv:2602.09097 \[hep-ph\]](#).
- [10] **Super-Kamiokande** Collaboration, A. Takenaka *et al.*, “Search for proton decay via $p \rightarrow e^+ \pi^0$ and $p \rightarrow \mu^+ \pi^0$ with an enlarged fiducial volume in Super-Kamiokande I-IV,” *Phys. Rev. D* **102** no. 11, (2020) 112011, [arXiv:2010.16098 \[hep-ex\]](#).
- [11] **Hyper-Kamiokande** Collaboration, K. Abe *et al.*, “Hyper-Kamiokande Design Report,” [arXiv:1805.04163 \[physics.ins-det\]](#).
- [12] **DUNE** Collaboration, B. Abi *et al.*, “Deep Underground Neutrino Experiment (DUNE), Far Detector Technical Design Report, Volume II: DUNE Physics,” [arXiv:2002.03005 \[hep-ex\]](#).
- [13] **JUNO** Collaboration, A. Abusleme *et al.*, “JUNO physics and detector,” *Prog. Part. Nucl. Phys.* **123** (2022) 103927, [arXiv:2104.02565 \[hep-ex\]](#).
- [14] J. C. Helo, M. Hirsch, and T. Ota, “Proton decay at one loop,” *Phys. Rev. D* **99** no. 9, (2019) 095021, [arXiv:1904.00036 \[hep-ph\]](#).
- [15] Z.-j. Tao, “Radiative seesaw mechanism at weak scale,” *Phys.Rev.D* **54** (1996) 5693–5697, [arXiv:hep-ph/9603309 \[hep-ph\]](#).
- [16] E. Ma, “Verifiable radiative seesaw mechanism of neutrino mass and dark matter,” *Phys. Rev. D* **73** (2006) 077301, [arXiv:hep-ph/0601225](#).
- [17] T. Nomura and O. Popov, “Extended scotogenic model of neutrino mass and proton decay,” *Phys. Rev. D* **110** no. 7, (2024) 075035, [arXiv:2406.00651 \[hep-ph\]](#).
- [18] S. K. Kang and O. Popov, “Pathways to proton’s stability via naturally small neutrino masses,” [arXiv:2412.20723 \[hep-ph\]](#).
- [19] R. Kumar and R. Srivastava, “Dark matter induced proton decays,” *JHEP* **04** (2026) 024, [arXiv:2506.04370 \[hep-ph\]](#).
- [20] J. M. Pendlebury *et al.*, “Revised experimental upper limit on the electric dipole moment of the neutron,” *Phys. Rev. D* **92** no. 9, (2015) 092003, [arXiv:1509.04411 \[hep-ex\]](#).
- [21] C. A. Baker *et al.*, “An Improved experimental limit on the electric dipole moment of the neutron,” *Phys. Rev. Lett.* **97** (2006) 131801, [arXiv:hep-ex/0602020](#).
- [22] R. D. Peccei and H. R. Quinn, “CP Conservation in the Presence of Instantons,” *Phys. Rev. Lett.* **38** (1977) 1440–1443.
- [23] R. D. Peccei and H. R. Quinn, “Constraints Imposed by CP Conservation in the Presence of Instantons,” *Phys. Rev. D* **16** (1977) 1791–1797.
- [24] S. Weinberg, “A New Light Boson?,” *Phys. Rev. Lett.* **40** (1978) 223–226.
- [25] F. Wilczek, “Problem of Strong P and T Invariance in the Presence of Instantons,” *Phys. Rev. Lett.* **40** (1978) 279–282.
- [26] A. R. Zhitnitsky, “On Possible Suppression of the Axion Hadron Interactions. (In Russian),” *Sov. J. Nucl. Phys.* **31** (1980)

260.

- [27] M. Dine, W. Fischler, and M. Srednicki, “A Simple Solution to the Strong CP Problem with a Harmless Axion,” *Phys. Lett. B* **104** (1981) 199–202.
- [28] J. E. Kim, “Weak Interaction Singlet and Strong CP Invariance,” *Phys. Rev. Lett.* **43** (1979) 103.
- [29] M. A. Shifman, A. I. Vainshtein, and V. I. Zakharov, “Can Confinement Ensure Natural CP Invariance of Strong Interactions?,” *Nucl. Phys. B* **166** (1980) 493–506.
- [30] L. Di Luzio, M. Giannotti, E. Nardi, and L. Visinelli, “The landscape of QCD axion models,” *Phys. Rept.* **870** (2020) 1–117, [arXiv:2003.01100 \[hep-ph\]](#).
- [31] J. Preskill, M. B. Wise, and F. Wilczek, “Cosmology of the Invisible Axion,” *Phys. Lett. B* **120** (1983) 127–132.
- [32] L. F. Abbott and P. Sikivie, “A Cosmological Bound on the Invisible Axion,” *Phys. Lett. B* **120** (1983) 133–136.
- [33] M. Dine and W. Fischler, “The Not So Harmless Axion,” *Phys. Lett. B* **120** (1983) 137–141.
- [34] P. Minkowski, “ $\mu \rightarrow e\gamma$ at a Rate of One Out of 10^9 Muon Decays?,” *Phys. Lett. B* **67** (1977) 421–428.
- [35] M. Gell-Mann, P. Ramond, and R. Slansky, “Complex Spinors and Unified Theories,” *Conf. Proc. C* **790927** (1979) 315–321, [arXiv:1306.4669 \[hep-th\]](#).
- [36] T. Yanagida, “Horizontal gauge symmetry and masses of neutrinos,” *Conf. Proc. C* **7902131** (1979) 95–99.
- [37] J. Schechter and J. W. F. Valle, “Neutrino Masses in $SU(2) \times U(1)$ Theories,” *Phys. Rev. D* **22** (1980) 2227.
- [38] S. L. Glashow, “The Future of Elementary Particle Physics,” *NATO Sci. Ser. B* **61** (1980) 687.
- [39] R. N. Mohapatra and G. Senjanovic, “Neutrino Mass and Spontaneous Parity Nonconservation,” *Phys. Rev. Lett.* **44** (1980) 912.
- [40] R. R. Volkas, A. J. Davies, and G. C. Joshi, “NATURALNESS OF THE INVISIBLE AXION MODEL,” *Phys. Lett. B* **215** (1988) 133–138.
- [41] J. D. Clarke and R. R. Volkas, “Technically natural nonsupersymmetric model of neutrino masses, baryogenesis, the strong CP problem, and dark matter,” *Phys. Rev. D* **93** no. 3, (2016) 035001, [arXiv:1509.07243 \[hep-ph\]](#).
- [42] A. H. Sopov and R. R. Volkas, “VISH ν : a unified solution to five SM shortcomings with a protected electroweak scale,” [arXiv:2206.11598 \[hep-ph\]](#).
- [43] R. R. Volkas, “VISH ν : Flavour-Variant DFSZ Axion Model for Inflation, Neutrino Masses, Dark Matter, and Baryogenesis,” *LHEP* **2023** (2023) 358.
- [44] M. Matlis, J. Dutta, G. Moortgat-Pick, and A. Ringwald, “Inflation and Higgs phenomenology in a model unifying the DFSZ axion with the majoron,” *JCAP* **07** (2024) 007, [arXiv:2309.10857 \[hep-ph\]](#).
- [45] A. Salvio, “A Simple Motivated Completion of the Standard Model below the Planck Scale: Axions and Right-Handed Neutrinos,” *Phys. Lett. B* **743** (2015) 428–434, [arXiv:1501.03781 \[hep-ph\]](#).
- [46] G. Ballesteros, J. Redondo, A. Ringwald, and C. Tamarit, “Unifying inflation with the axion, dark matter, baryogenesis and the seesaw mechanism,” *Phys. Rev. Lett.* **118** no. 7, (2017) 071802, [arXiv:1608.05414 \[hep-ph\]](#).
- [47] G. Ballesteros, J. Redondo, A. Ringwald, and C. Tamarit, “Standard Model—axion—seesaw—Higgs portal inflation. Five problems of particle physics and cosmology solved in one stroke,” *JCAP* **08** (2017) 001, [arXiv:1610.01639 \[hep-ph\]](#).
- [48] J. R. Rocha, H. B. Camara, and F. R. Joaquim, “Flavored Peccei-Quinn symmetries in the minimal ν DFSZ model,” *Phys. Rev. D* **112** no. 7, (2025) 075053, [arXiv:2504.00088 \[hep-ph\]](#).
- [49] A. Batra, H. B. Camara, F. R. Joaquim, R. Srivastava, and J. W. F. Valle, “Axion Paradigm with Color-Mediated Neutrino Masses,” *Phys. Rev. Lett.* **132** no. 5, (2024) 051801, [arXiv:2309.06473 \[hep-ph\]](#).
- [50] A. Batra, H. B. Camara, F. R. Joaquim, N. Nath, R. Srivastava, and J. W. F. Valle, “Axion framework with color-mediated Dirac neutrino masses,” *Phys. Lett. B* **868** (2025) 139629, [arXiv:2501.13156 \[hep-ph\]](#).
- [51] M. Reig and R. Srivastava, “Spontaneous proton decay and the origin of Peccei-Quinn symmetry,” *Phys. Lett. B* **790** (2019) 134–139, [arXiv:1809.02093 \[hep-ph\]](#).
- [52] R. M. Fonseca, M. Hirsch, and R. Srivastava, “ $\Delta L = 3$ processes: Proton decay and the LHC,” *Phys. Rev. D* **97** no. 7, (2018) 075026, [arXiv:1802.04814 \[hep-ph\]](#).
- [53] G. Grilli di Cortona, E. Hardy, J. Pardo Vega, and G. Villadoro, “The QCD axion, precisely,” *JHEP* **01** (2016) 034, [arXiv:1511.02867 \[hep-ph\]](#).
- [54] **Super-Kamiokande** Collaboration, N. Taniuchi *et al.*, “Search for proton decay via $p \rightarrow e + \eta$ and $p \rightarrow \mu + \eta$ with a 0.37 Mton-year exposure of Super-Kamiokande,” *Phys. Rev. D* **110** no. 11, (2024) 112011, [arXiv:2409.19633 \[hep-ex\]](#).
- [55] **Super-Kamiokande** Collaboration, K. Abe *et al.*, “Search for nucleon decay into charged antilepton plus meson in 0.316 megaton-years exposure of the Super-Kamiokande water Cherenkov detector,” *Phys. Rev. D* **96** no. 1, (2017) 012003,

- [arXiv:1705.07221 \[hep-ex\]](#).
- [56] **Super-Kamiokande** Collaboration, R. Matsumoto *et al.*, “Search for proton decay via $p \rightarrow \mu^+ K^0$ in 0.37 megaton-years exposure of Super-Kamiokande,” *Phys. Rev. D* **106** no. 7, (2022) 072003, [arXiv:2208.13188 \[hep-ex\]](#).
- [57] **Particle Data Group** Collaboration, S. Navas *et al.*, “Review of particle physics,” *Phys. Rev. D* **110** no. 3, (2024) 030001.
- [58] Y. Aoki, T. Izubuchi, E. Shintani, and A. Soni, “Improved lattice computation of proton decay matrix elements,” *Phys. Rev. D* **96** no. 1, (2017) 014506, [arXiv:1705.01338 \[hep-lat\]](#).
- [59] T. Li, M. A. Schmidt, and C.-Y. Yao, “Baryon-number-violating nucleon decays in ALP effective field theories,” *JHEP* **08** (2024) 221, [arXiv:2406.11382 \[hep-ph\]](#).
- [60] W.-Q. Fan, Y. Liao, X.-D. Ma, and H.-L. Wang, “Comprehensive investigation on baryon number violating nucleon decays involving an axion-like particle*,” *Chin. Phys. C* **50** no. 3, (2026) 033103, [arXiv:2507.11844 \[hep-ph\]](#).
- [61] **Planck** Collaboration, N. Aghanim *et al.*, “Planck 2018 results. VI. Cosmological parameters,” *Astron. Astrophys.* **641** (2020) A6, [arXiv:1807.06209 \[astro-ph.CO\]](#). [Erratum: *Astron. Astrophys.* 652, C4 (2021)].
- [62] M. Beltran, J. Garcia-Bellido, and J. Lesgourgues, “Isocurvature bounds on axions revisited,” *Phys. Rev. D* **75** (2007) 103507, [arXiv:hep-ph/0606107](#).
- [63] L. Di Luzio, F. Mescia, and E. Nardi, “Redefining the Axion Window,” *Phys. Rev. Lett.* **118** no. 3, (2017) 031801, [arXiv:1610.07593 \[hep-ph\]](#).
- [64] P. W. Graham and D. Racco, “Revisiting isocurvature bounds on the minimal QCD axion,” *JHEP* **12** (2025) 028, [arXiv:2506.03348 \[hep-ph\]](#).
- [65] D. P. Bennett and F. R. Bouchet, “Evidence for a Scaling Solution in Cosmic String Evolution,” *Phys. Rev. Lett.* **60** (1988) 257.
- [66] D. G. Levkov, A. G. Panin, and I. I. Tkachev, “Gravitational Bose-Einstein condensation in the kinetic regime,” *Phys. Rev. Lett.* **121** no. 15, (2018) 151301, [arXiv:1804.05857 \[astro-ph.CO\]](#).
- [67] M. Gorghetto, E. Hardy, and G. Villadoro, “Axions from Strings: the Attractive Solution,” *JHEP* **07** (2018) 151, [arXiv:1806.04677 \[hep-ph\]](#).
- [68] M. Buschmann, J. W. Foster, and B. R. Safdi, “Early-Universe Simulations of the Cosmological Axion,” *Phys. Rev. Lett.* **124** no. 16, (2020) 161103, [arXiv:1906.00967 \[astro-ph.CO\]](#).
- [69] G. Lazarides, M. Reig, Q. Shafi, R. Srivastava, and J. W. F. Valle, “Spontaneous Breaking of Lepton Number and the Cosmological Domain Wall Problem,” *Phys. Rev. Lett.* **122** no. 15, (2019) 151301, [arXiv:1806.11198 \[hep-ph\]](#).
- [70] M. Kawasaki, K. Saikawa, and T. Sekiguchi, “Axion dark matter from topological defects,” *Phys. Rev. D* **91** no. 6, (2015) 065014, [arXiv:1412.0789 \[hep-ph\]](#).
- [71] V. B. . Klaer and G. D. Moore, “The dark-matter axion mass,” *JCAP* **11** (2017) 049, [arXiv:1708.07521 \[hep-ph\]](#).
- [72] M. Gorghetto, E. Hardy, and G. Villadoro, “More axions from strings,” *SciPost Phys.* **10** no. 2, (2021) 050, [arXiv:2007.04990 \[hep-ph\]](#).
- [73] M. Buschmann, J. W. Foster, A. Hook, A. Peterson, D. E. Willcox, W. Zhang, and B. R. Safdi, “Dark matter from axion strings with adaptive mesh refinement,” *Nature Commun.* **13** no. 1, (2022) 1049, [arXiv:2108.05368 \[hep-ph\]](#).
- [74] J. N. Benabou, M. Buschmann, J. W. Foster, and B. R. Safdi, “Axion Mass Prediction from Adaptive Mesh Refinement Cosmological Lattice Simulations,” *Phys. Rev. Lett.* **134** no. 24, (2025) 241003, [arXiv:2412.08699 \[hep-ph\]](#).
- [75] P. Sikivie, “Of Axions, Domain Walls and the Early Universe,” *Phys. Rev. Lett.* **48** (1982) 1156–1159.
- [76] R. Roshan and G. White, “Using gravitational waves to see the first second of the Universe,” *Rev. Mod. Phys.* **97** no. 1, (2025) 015001, [arXiv:2401.04388 \[hep-ph\]](#).
- [77] G. Servant and P. Simakachorn, “Constraining postinflationary axions with pulsar timing arrays,” *Phys. Rev. D* **108** no. 12, (2023) 123516, [arXiv:2307.03121 \[hep-ph\]](#).
- [78] A. P. Morais, V. Oliveira, A. Onofre, R. Pasechnik, and R. Santos, “Exploring the viability of a pseudo-Nambu-Goldstone boson as ultralight dark matter in a mass range relevant for strong gravity applications,” *Phys. Rev. D* **110** no. 3, (2024) 035008, [arXiv:2305.03776 \[hep-ph\]](#).
- [79] E. Nardi and E. Roulet, “Are exotic stable quarks cosmologically allowed?,” *Phys. Lett. B* **245** (1990) 105–110.
- [80] M. L. Perl, P. C. Kim, V. Halvo, E. R. Lee, I. T. Lee, D. Loomba, and K. S. Lackner, “The Search for stable, massive, elementary particles,” *Int. J. Mod. Phys. A* **16** (2001) 2137–2164, [arXiv:hep-ex/0102033](#).
- [81] M. L. Perl, E. R. Lee, and D. Loomba, “Searches for fractionally charged particles,” *Ann. Rev. Nucl. Part. Sci.* **59** (2009) 47–65.
- [82] S. Burdin, M. Fairbairn, P. Mermod, D. Milstead, J. Pinfold, T. Sloan, and W. Taylor, “Non-collider searches for stable

- massive particles,” *Phys. Rept.* **582** (2015) 1–52, [arXiv:1410.1374 \[hep-ph\]](#).
- [83] M. P. Hertzberg and A. Masoumi, “Astrophysical Constraints on Singlet Scalars at LHC,” *JCAP* **04** (2017) 028, [arXiv:1607.06445 \[hep-ph\]](#).
- [84] G. D. Mack, J. F. Beacom, and G. Bertone, “Towards Closing the Window on Strongly Interacting Dark Matter: Far-Reaching Constraints from Earth’s Heat Flow,” *Phys. Rev. D* **76** (2007) 043523, [arXiv:0705.4298 \[astro-ph\]](#).
- [85] L. Di Luzio, F. Mescia, and E. Nardi, “Window for preferred axion models,” *Phys. Rev. D* **96** no. 7, (2017) 075003, [arXiv:1705.05370 \[hep-ph\]](#).
- [86] **CAST** Collaboration, V. Anastassopoulos *et al.*, “New CAST Limit on the Axion-Photon Interaction,” *Nature Phys.* **13** (2017) 584–590, [arXiv:1705.02290 \[hep-ex\]](#).
- [87] **ADMX** Collaboration, N. Du *et al.*, “A Search for Invisible Axion Dark Matter with the Axion Dark Matter Experiment,” *Phys. Rev. Lett.* **120** no. 15, (2018) 151301, [arXiv:1804.05750 \[hep-ex\]](#).
- [88] **ADMX** Collaboration, T. Braine *et al.*, “Extended Search for the Invisible Axion with the Axion Dark Matter Experiment,” *Phys. Rev. Lett.* **124** no. 10, (2020) 101303, [arXiv:1910.08638 \[hep-ex\]](#).
- [89] **ADMX** Collaboration, C. Bartram *et al.*, “Search for Invisible Axion Dark Matter in the 3.3–4.2 μeV Mass Range,” *Phys. Rev. Lett.* **127** no. 26, (2021) 261803, [arXiv:2110.06096 \[hep-ex\]](#).
- [90] S. De Panfilis, A. C. Melissinos, B. E. Moskowitz, J. T. Rogers, Y. K. Semertzidis, W. Wuensch, H. J. Halama, A. G. Prodel, W. B. Fowler, and F. A. Nezrick, “Limits on the Abundance and Coupling of Cosmic Axions at 4.5-Microev $< m(a) < 5.0$ -Microev,” *Phys. Rev. Lett.* **59** (1987) 839.
- [91] **CAPP** Collaboration, O. Kwon *et al.*, “First Results from an Axion Haloscope at CAPP around 10.7 μeV ,” *Phys. Rev. Lett.* **126** no. 19, (2021) 191802, [arXiv:2012.10764 \[hep-ex\]](#).
- [92] **HAYSTAC** Collaboration, K. M. Backes *et al.*, “A quantum-enhanced search for dark matter axions,” *Nature* **590** no. 7845, (2021) 238–242, [arXiv:2008.01853 \[quant-ph\]](#).
- [93] I. Shilon, A. Dudarev, H. Silva, and H. H. J. ten Kate, “Conceptual design of a new large superconducting toroid for IAXO, the new international AXion observatory,” *IEEE Transactions on Applied Superconductivity* **23** no. 3, (2013) 4500604–4500604. <https://doi.org/10.1109/2Ftasc.2013.2251052>.
- [94] I. Stern, “ADMX Status,” *PoS ICHEP2016* (2016) 198, [arXiv:1612.08296 \[physics.ins-det\]](#).
- [95] S. Beurthey *et al.*, “MADMAX Status Report,” [arXiv:2003.10894 \[physics.ins-det\]](#).
- [96] **ALPHA** Collaboration, A. J. Millar *et al.*, “Searching for dark matter with plasma haloscopes,” *Phys. Rev. D* **107** no. 5, (2023) 055013, [arXiv:2210.00017 \[hep-ph\]](#).
- [97] J. L. Ouellet *et al.*, “First Results from ABRACADABRA-10 cm: A Search for Sub- μeV Axion Dark Matter,” *Phys. Rev. Lett.* **122** no. 12, (2019) 121802, [arXiv:1810.12257 \[hep-ex\]](#).
- [98] M. Lawson, A. J. Millar, M. Pancaldi, E. Vitagliano, and F. Wilczek, “Tunable axion plasma haloscopes,” *Phys. Rev. Lett.* **123** no. 14, (2019) 141802, [arXiv:1904.11872 \[hep-ph\]](#).
- [99] M. Wooten, A. Droster, A. Kenany, D. Sun, S. M. Lewis, and K. van Bibber, “Exploration of Wire Array Metamaterials for the Plasma Axion Haloscope,” *Annalen Phys.* **536** no. 1, (2024) 2200479, [arXiv:2203.13945 \[hep-ex\]](#).